



HAL
open science

Straightforward metal-free synthesis of an azacalix[6]arene forming a host–guest complex with fullerene C 60

Zhongrui Chen, Gabriel Canard, Cloé Azarias, Denis Jacquemin, Olivier Siri

► **To cite this version:**

Zhongrui Chen, Gabriel Canard, Cloé Azarias, Denis Jacquemin, Olivier Siri. Straightforward metal-free synthesis of an azacalix[6]arene forming a host–guest complex with fullerene C 60. *New Journal of Chemistry*, 2017, 41 (13), pp.5284 - 5290. 10.1039/c7nj00697g . hal-01783783

HAL Id: hal-01783783

<https://amu.hal.science/hal-01783783>

Submitted on 4 May 2018

HAL is a multi-disciplinary open access archive for the deposit and dissemination of scientific research documents, whether they are published or not. The documents may come from teaching and research institutions in France or abroad, or from public or private research centers.

L'archive ouverte pluridisciplinaire **HAL**, est destinée au dépôt et à la diffusion de documents scientifiques de niveau recherche, publiés ou non, émanant des établissements d'enseignement et de recherche français ou étrangers, des laboratoires publics ou privés.

Straightforward Metal-Free Synthesis of an Azacalix[6]arene Forming a Host-Guest Complex with Fullerene C₆₀

Zhongrui Chen,^a Gabriel Canard,^{*a} Cloé Azarias,^b Denis Jacquemin^{*b,c} and Olivier Siri^{*a}

Contrasting with the well mastered azacalix[4]arene, the synthesis and characterization of azacalix[6]arene derivatives remains a challenge for chemists. In this framework, bulky *n*-octylamino groups appended on the 1,3-*meta*-diaminobenzene **2b** can lead to the concomitant and straightforward one-pot formation of the azacalix[6]arene **4b** and of the thermodynamically favoured azacalix[4]arene **3b** through simple consecutive nucleophilic aromatic substitutions. The conformations of **3b** and **4b** were studied in solution and in the solid state using their molecular structures, their NMR and UV-visible spectra combined with first principle TD-DFT calculations. Preliminary solution experiments show that **4b** can form a 1:1 host-guest complex with C₆₀.

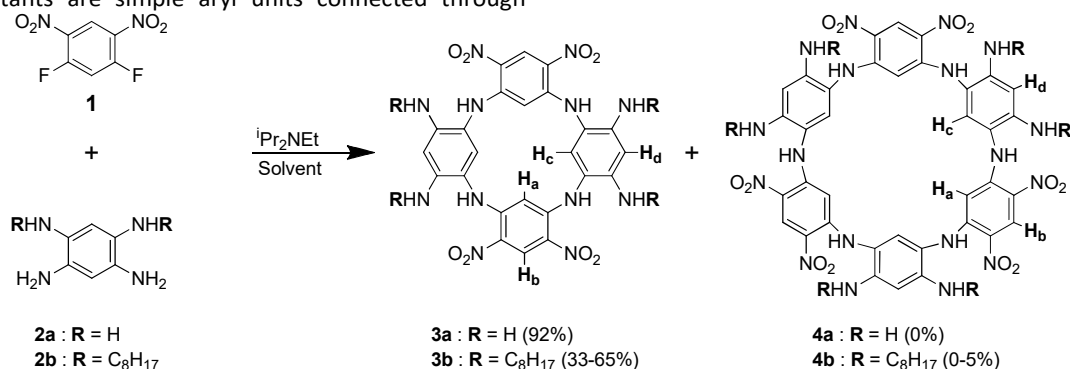
Introduction

Since their first complete characterization in the early 1970s, calixarenes have become the subject of an intense research and have been applied in various fields such as catalysis and specific delivery of drugs.¹ Among the different ways to tune the cavity sizes and shapes of these macrocycles, one can focus on the connection between aryl units by heteroatoms thereby forming heterocalixarenes.² Compared to thiacalixarenes incorporating sulfur-bridging atoms that were intensively studied,³ the research devoted to the syntheses and applications of an emerging class of heterocalixarenes, namely, azacalixarenes is still in its infancy.⁴ This class of calixarenes are of peculiar interest because the connecting nitrogen atoms may bring supplementary functionalities to the macrocycle. For instance, the nitrogen atoms can form supramolecular bonds and their alkylation was used to produce derivatives with an improved solubility and/or featuring an inherent chirality.⁵ Moreover, electron rich polyazacyclophanes can be used as macrocyclic scaffolds for hole- and spin-containing molecular-based electronics.⁶

The synthesis of azacalixarenes relies on two principal strategies. The first one is the use of successive Buchwald-Hartwig palladium based aryl aminations that can produce azacalixarenes containing from three to more than ten building aryl or heteroaryl units.^{4,7} Another catalyst-free synthetic preparation of such azacyclophanes can be achieved using successive Nucleophilic Aromatic Substitutions (SNAr).^{4,8} This strategy was shown to produce only azacalix[4]arenes when the starting reactants are simple aryl units connected through

their *meta*-positions.^{4,8} In this case, the experimental conditions are probably responsible of the exclusive formation of the thermodynamically favoured *meta*-linked azacalix[4]arenes. Interestingly, the importance of using a kinetic vs. thermodynamic control during successive SNAr was illustrated for oxacalixarenes when studying the competing formation of poly(*m*-phenylene oxides) vs. *m*-cyclooligomers starting from the condensation of *meta*-dihydroxy- and *meta*-dihalo-aryl units⁹ which often affords oxacalix[4]arenes rather selectively over other larger macrocycles.¹⁰ Besides the use of non-equilibrating conditions,¹¹ the synthesis of large *m*-oxacalix[*n*]arenes (*n* > 4) by convenient SNAr strategies can be achieved following fragment coupling approaches¹² or by introducing bulky groups in the core of the cyclophanes.^{11b,13} To the best of our knowledge, such metal-free syntheses from simple aryl units are not yet described when considering large azacalix[*n*]arenes (*n* > 4) where the expansion of the cavity could bring, for example, unique recognition properties¹⁴ or a peculiar interaction with G-quadruplexes.¹⁵

The present work illustrates how two peripheral octyl chains appended on a 2,4-positions in tetraminobenzene can lead to the formation of an azacalix[6]arene by following a SNAr strategy using simple aryl units. This unprecedented azacyclophane is easily separated by chromatography from the large amounts of the thermodynamically favoured four member macrocycle that is concomitantly produced. A structural investigation of their respective conformation is conducted in the solid state and in solution using single crystal X-ray diffraction, NMR studies in connection with (time-dependent) density functional theory [(TD)-DFT] calculations.



Scheme 1 Synthesis of azacalix[4]arenes **3a-b** and of the azacalix[6]arene **4b**.

These first-principles calculations are combined with preliminary experiments to enlighten the impact of the macrocycle expansion towards the complexation of [60]fullerene.

Results and discussion

Concomitant formations of the azacalix[6]arene **4b** and the azacalix[4]arene **3b**.

A few years ago, we reported the synthesis of the tetraamino-azacalix[4]arene **3a** produced by the SNAr between the electron-deficient aryl **1** and 1,2,4,5-tetraminobenzene **2a** in MeCN in the presence of an excess of ⁱPr₂NEt acting as a non-nucleophilic base (Scheme 1).¹⁶ This one step strategy can be used to prepare N-substituted derivatives such as the tetra-*n*-octylamino-azacalix[4]arene **3b** starting from the N-substituted tetra-aminobenzene **2b** even if a two step procedure was shown to be more efficient (Scheme 1).¹⁷ The condensation of **1** and **2a** affords a single macrocycle **3a** irrespective of the experimental conditions with a very high yield reaching 92% when the reactant concentrations in MeCN is *ca.* 0.01 M. The macrocyclisation of the [2+2] product is probably favoured by intramolecular N-H...O₂N hydrogen bonding interactions involving the NH bridges that pre-organise the intermediate oligomers towards the cyclisation.^{8a}

Assuming that this pre-organisation would be rather disfavoured if N-substituents are added to the nucleophile **2** and knowing that the production of larger macrocycles is usually increased in more diluted conditions, a first experiment was conducted within the same conditions but using a twice diluted concentration of **2b** (Table 1, entry 1). If the cyclic tetramer **3b** appeared to be still the major reaction product, we could isolate a significant amount of the hexamer **4b** with a yield of 3.4% and with a simple chromatographic purification facilitated by the quite different polarities of the two macrocycles on silica (see the experimental section). The highest yield of **4b** reached 4.5% when pursuing the dilution of the reaction mixture (Table 2, entry 2) while, as expected, more concentrated conditions leads to a higher **3b/4b** ratio (Table 1, entries 3-4). We underline that highly ethanol-concentrated mixtures produce only linear oligomers and polymers because this solvent, by weakening the intramolecular hydrogen bonds, prevent the pre-organisation of oligomers towards the cyclisation (Table 1, entry 5).

Table 1 Screening of reaction conditions (using 1 equivalent of **2b**).

Entry	1 ^a	Solvent	[2b] (M)	ⁱ Pr ₂ NEt ^b	Temp. (°C)	3b/4b Yields (%)
1	0.95	MeCN	0.02	6	i) 0 °C (2 h) ii) rt. (12 h) iii) reflux (5 h)	32.4/3.4
2	0.95	MeCN	0.03	6	i) 0 °C (3 h) ii) rt. (120 h)	44.4/4.5
3	0.77	MeCN	0.11	10	i) 0 °C (4 h) ii) rt. (72 h)	60.5/2.6

4	0.95	ⁱ Pr ₂ NEt	0.86	7	iii) reflux (12 h) i) rt. (15 min) ii) 120 °C (72 h)	38.8/tr
5	0.90	EtOH	0.92	6	i) 0 °C (3 h) ii) rt (120 h)	-/-

^a Equivalents of **1**. ^b Equivalents of base.

Solid state conformations of **3b** and **4b**.

Despite the growth of numerous single crystals from different concentrated solutions of **3b** and **4b**, their molecular structures were all suffering from partial disorder affecting the long alkyl moieties and the co-crystallized solvent molecules. Nevertheless, we are still confident that the corresponding structural solutions and data refinements are of high enough qualities to allow us a first qualitative examination of their respective conformations in the solid state.

The crystal structure of **3b** features a typical 1,3-alternate conformation that is commonly observed in the structure of all the azacalix[4]arenes built on two equivalents of **1** (Figure 1).^{8c,8f,16b} This conformation, is also found by DFT as the most stable (*vide infra*), and is resulting from two stabilizing factors. The first one is the sp² character of the nitrogen bridging atoms that are conjugated with their adjacent electron-withdrawing dinitrobenzene rings illustrated by the short corresponding N–C bond lengths averaging 1.35 Å. The second one is the formation of four strong and intramolecular N-H...O₂N hydrogen bonds (average distance of 2.03 Å) that involve the acidic and bridging N-H moieties (Figure 1). Interestingly, this molecular arrangement induces the location of the two aromatic protons H_a of the dinitroaryl units (Scheme 1) in the anisotropic shielding cones of the two nearly parallel oriented (interplane angle of 4°) tetra-aminobenzene separated by 4.74 Å.

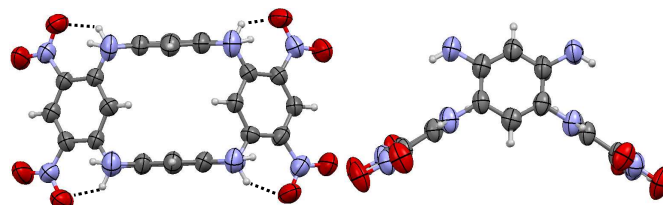


Fig 1. Two views of the single-crystal X-ray structure of **3b** (N-octyl chains are omitted for clarity). The dotted lines show the intramolecular NH...O₂N hydrogen bonds.

Very few examples of single crystal X-ray structures of azacalix[6]arenes were reported previously. In 2006, Vale *et al.* described the structure of an aza[6]metacyclophane bearing six *p*-*tert*-butylphenyl groups in a 1,3,5-alternate conformation with an approximate S₆ point group of symmetry.^{7d} Two years later, an analogous derivative bearing six supplementary methoxy groups was shown to adopt, in the solid state, a definite 1,2,3-alternate conformation stabilized by intramolecular hydrogen bonds.¹⁸ In 2002 and 2005, Yamamoto *et al.* reported the crystal structure of an azacalix[6]heteroarene adopting a triangular shape in which each of the six pyridine rings were alternatively inclined upward and downward to the macrocyclic plane due to the electrostatic repulsion between

the lone pairs of the N-pyridine and of the N-bridging atoms.^{7b,19}

Two molecules featuring the same conformation are contained in the asymmetric unit of the crystal structure of **4b** (Figure 2). At first glance, **4b** adopts an 1,2,4,5 alternate (u,d,d,u,d,d) conformation^{1a,20} which no remarkable symmetry element. Because of the two different building blocks, each kind of fragments is found in the two aryl groups that are orientated upward. The molecular cavity is rendered inaccessible to solvent molecules by the upward tetra-amino benzene unit. This latter aryl group is probably folding inside the cavity following two weak CH...N hydrogen bonds that cannot be precisely determined regarding the low resolution of the structure. As we show below, theoretical calculations deliver a very similar conformation as the most stable amongst those tested. Interestingly, if this conformation was kept frozen in solution, one would expect two different sets of signals for each kind of aromatic protons. For example, as in the structure of **3b**, the aromatic proton H_a (Scheme 1) of the upward dinitroaryl moiety is in the anisotropic shielding cones of the adjacent downward orientated and nearly parallel tetra-aminobenzene moieties while the two other equivalent H_a protons are only affected by one shielding cone.

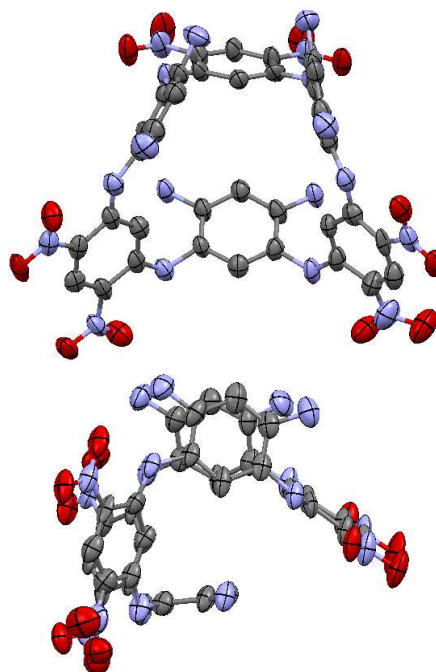


Fig 2. Two views of the single-crystal X-ray structure of **4b** (N-octyl chains and solvent molecules are omitted for clarity, the hydrogen atoms locations were not fitted).

Conformations of **3b** and **4b** in solution.

A first insight of the conformations of **3b** and **4b** in solutions is given by their ¹H NMR spectra recorded in CDCl₃ at room temperature (Figure 3). The azacalix[4]arene **3b** has a single and symmetrical 1,3-alternate conformer in which the intramolecular aromatic protons H_a are located inside the anisotropic shielding cone of the two adjacent aryl rings. This particular effect is put into evidence by the corresponding singlet at a high field chemical shift of $\delta = 5.49$ ppm. As stated above, this conformation is stabilized by four NH...O₂N hydrogen bonds that are illustrated by the down-field signal of the bridging NH signals at $\delta = 8.85$ ppm. The assignments of the NMR signals of **3b** are also consistent with theoretical calculations (see the ESI). As for **3b**, the ¹H HMR spectrum of the larger macrocycle **4b** features only one signal for each aromatic and NH protons (Figure 3).

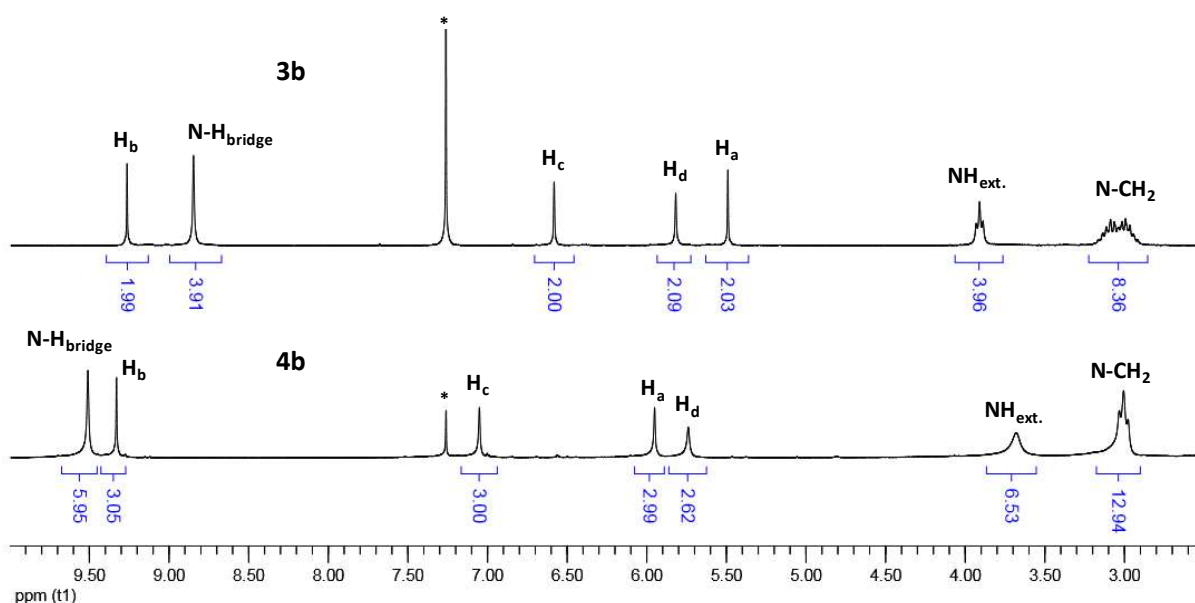


Fig 3. Partial ^1H NMR spectra of **3b** and **4b** recorded in CDCl_3 at room temperature (asterisks denote residual solvent peaks; the full spectra are given in the SI).

This result underlines that **4b** either adopts a symmetrical favourite conformation in solution or that this spectrum is resulting from different equivalent or non-equivalent structures that are rapidly interconverting on the NMR time scale.

The UV-Visible spectrum of a diluted dichloromethane solution of **3b** (Figure 4) is characterized by an intense band in the UV region (340 nm) together with a shoulder lying at lower energy (400 nm). These bands originate from $\pi\text{-}\pi^*$ transitions of the electronically independent diamino-dinitro-benzene units as shown previously by TD-DFT calculations performed on similar derivatives.^{8h} A noticeable consequence of the macrocycle's expansion is evidenced by the corresponding absorption spectrum of **4b** (Figure 4) displaying two bands, though having maxima located at equal energies, that have a different intensity ratio. Moreover, the ring expansion induces the broadening of the visible band that extends up to 600 nm. This effect can be attributed to an effective π -conjugation between two consecutive aryl units in **4b** which is, in contrast, interrupted by the restricted and "frozen" 1,3 alternate conformation of **3b**.²¹

We have searched the conformational space for both **3b** and **4b** using DFT calculations. For the former, DFT predicts that the 1,3-alternate conformation is the most stable, the following one being at least more than 10 $\text{kcal}\cdot\text{mol}^{-1}$ less stable (see the ESI for details). Interestingly, despite the fact that a greater conformational flexibility would be expected for **4b**, DFT provides exactly the same conclusion as for **3b**: the conformer corresponding to the XRD structure is much more stable than the others. Together with the experimental NMR spectra, this indicates that there is probably an interconversion of **4b** between equivalent structures alike the one displayed in Figure 2. This analysis is also supported by a comparison between theoretical and experimental NMR chemical shifts (see the ESI).

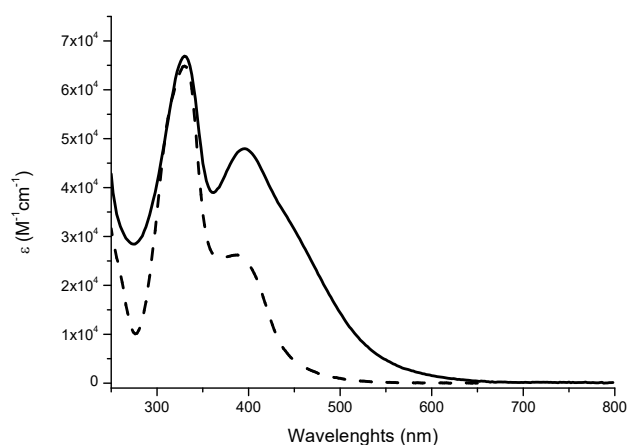


Fig 4. UV-Visible spectra of diluted dichloromethane solutions of **3b** (dashed line) and **4b** (solid line).

When comparing the experimental and theoretical UV/Vis spectra of **3b** (Figure S4 in the ESI,) one observes that, despite a blue-shift of the bands (of 0.25 eV and 0.27 eV for the short- and long-wavelength band, respectively), theory provides a shape that matches well the one of Figure 4. Indeed, though the relative intensity of the long-wavelength maxima is somehow underestimated, the theoretical separation between the two bands (0.55 eV) is in excellent agreement with the experimental value of 0.58 eV. The orbital composition of each relevant electronic transition, as well as the orbital shapes of **3b** can be found in the ESI. One can conclude from these data that the excitations responsible for both absorption bands of **3b** mainly imply molecular orbitals centered on the phenyl rings bearing the nitro groups, though there is small contribution from the phenyl rings bearing the amino groups for the longest wavelength band.

In Figures S6, we compare the experimental and theoretical spectra of **4b**. Even though the shape of the theoretical convoluted spectra does not perfectly match with the experimental curve, theory provides accurate trends. Indeed, when going from **3b** to **4b**, one notes: i) no important changes of the intense absorption at *ca.* 300 nm in both theoretical and measured spectra; ii) the spectrum of **4b** extends to larger wavelengths which also fits the experimental observation. Interestingly by analysing, the nature of this additional long-wavelength band specific to **4b**, one clearly notices that it corresponds to a charge-transfer band, as the key occupied MOs are localized on the amino-phenyl rings (donor) whereas their unoccupied counterparts are centered on the nitro-phenyl moieties (see Table S7 and Figure S7). Such transfer was not possible in **3b**, due to the orthogonal nature of the phenyl planes in that compound.

Complexation of C₆₀ by **3b** and **4b**.

Previous works have focused on the recognition properties of large azacalix[n]heteroarenes (n=5-10) towards guests such as fullerene derivatives.¹⁴ Consequently, we ran preliminary solution experiments to study if host-guest complexes are formed between C₆₀ and the azacalixarenes **3b** and **4b**. In tetrachloroethane solutions at a millimolar scale (0.4 mM), no interaction occurs between **3b** and increasing amounts of C₆₀ as illustrated by the corresponding UV-Visible spectra that result from a simple addition of the absorption spectra of each component (Figure S8 in the SI). On the contrary, when the same experiment was conducted using **4b**, a clear modification of the shape and intensity of the visible band was detected and reveal the probable formation of a 1:1 complexation through the presence of two isosbestic points (Figure S9).

We have performed DFT calculations on the possible complexes between C₆₀ and both **3b** and **4b**. The results are detailed in the ESI. For **3b**-C₆₀ the most stable aggregate that could be identified presents an interaction free energy as small as *ca.* -3 kcal.mol⁻¹. In contrast, for **4b**-C₆₀, we could found two complexes presenting interaction energies of *ca.* -9 kcal.mol⁻¹ compared to the corresponding **4b** free conformer (see Figure 5 and S16). In these two compounds, the C₆₀ is interacting with the nitro-phenyl moieties. Interestingly, we note that this interaction takes place with two rings for the most stable "free" conformer found in XRD (left-hand-side in Figure 5) or three rings for a less stable conformer (right-hand-side in Figure 5). For this latter case, the gain of interaction energy is however too limited to compensate the less stable character of the free conformer (10 kcal.mol⁻¹, see Table S2), and only the former is foreseen to be present in solution.

For the most stable **4b**-C₆₀ aggregate, we have determined the UV/Vis spectra with TD-DFT, using CAM-B3LYP, a functional known to provide a sound description of long-range charge-transfer excited-states. Compared to the free **4b**, these TD-DFT calculations revealed several additional transitions of weak intensity in the 450-500 nm domain, which fits the experimental findings (Figure S9). Amongst all these TD-DFT

vertical transitions, the most intense takes place at 474 nm (*f*=0.02) and the largest MO contribution to it is an HOMO to LUMO transitions. Those orbitals are displayed in Figure 6 and it is crystal clear that they imply a charge-transfer from the amino rings of **4b** (HOMO) to the C₆₀ (LUMO).

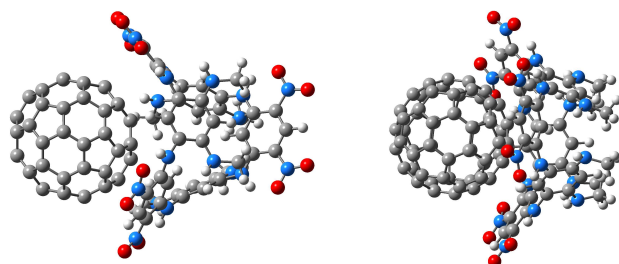


Fig 5. View of the two most stable **4b**-C₆₀ complexes identified by DFT calculations.

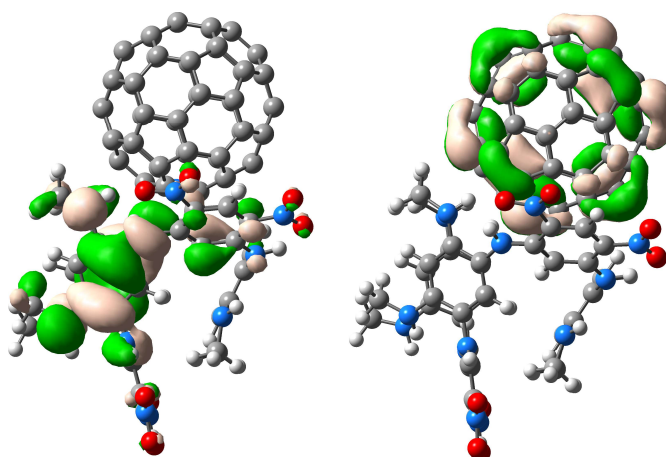


Fig 6. HOMO (left) and LUMO (right) of the most stable **4b**-C₆₀ aggregate.

Experimental

Materials and methods.

Compound **2b** was prepared according to literature procedure.¹⁷ All reagents and solvents anhydrate were purchased from Alfa Aesar or Sigma Aldrich and were used without further purification. Column chromatography was performed using silica gel (60-120 mesh). Analytical thin layer chromatography (TLC) was performed on precoated silica gel-60 F254 (0.5 mm) aluminium plate. Visualization of the spots on TLC plates was achieved by exposure to UV light. ¹H and ¹³C NMR spectra were recorded on a Bruker AC250 or on a JEOL ECS400 NMR spectrometer. Chemical shifts are reported in delta (δ) units, expressed in parts per million using the residual protonated solvent signal as an internal standard (For proton: CDCl₃, 7.26 ppm; Acetone-d₆, 2.05 ppm. For ¹³C: CDCl₃, 77.0 ppm; Acetone-d₆, 30.8 ppm. The multiplicity of the signals is designated by the following abbreviations: s, singlet; br s, broad singlet; d, doublet; t, triplet; br t, broad triplet; m, multiplet. Coupling constants, *J*, are reported in Hertz (Hz). High-resolution mass spectrometry (HRMS) analysis was performed on a SYNAPT G2 HDMS (Waters). Absorption spectra were recorded using 1 mm and 10 mm quartz cells in a

Varian Cary 50 UV-vis spectrophotometer and spectroscopic grade solvents.

Synthesis of compounds 3b and 4b. To a solution of 1,5-difluoro-2,4-dinitrobenzene **1** (m= 135 mg, 0.66 mmol, 0.95 equiv.) in anhydrous MeCN (7 mL), was added **2b** (m= 300 mg, 0.69 mmol, 1.0 equiv.). The flask was closed by a septum, and cooled in a water-ice bath. The system was degassed 3 times by pump-argon cycling. Under argon degassed DIPEA (720 μ L, 4.13 mmol, 6.0 equiv.) was added dropwise by a syringe. After stirring at 0 °C for 3 hrs, the solution was stirred at room temperature for 5 days. The resulting solid in suspension was filtered and rinsed with acetone (100 mL) affording **3b** (m= 127 mg, 121 μ mol) as an orange powder. The filtrate was concentrated under reduced pressure. The resulting residue was purified by column chromatography (silica 60F, DCM/cyclohexane, 70/30) to afford an additional quantity of **3b** (25.6 mg, 24.3 μ mol, overall yield of 44.4%) and **4b** as a dark greenish yellow powder (m= 16 mg, 9.9 μ mol, 5% yield). **3b**: R_f = 0.29; Other analytical data are consistent with literature data.¹⁷ Single diffracting crystals of **3b** were obtained by slow diffusion of *n*-heptane into a concentrated chloroform solution of **3b**. **4b**: R_f = 0.51; M.p. 253-255°C; ¹H NMR (250 MHz, Acetone-*d*₆): δ 9.58 (br s, 6H), 9.20 (s, 3H), 7.20 (s, 3H), 6.02 (s, 3H), 5.94 (s, 3H), 4.75 (br t, ³ J_{HH} = 5.7 Hz, 6H), 3.15 (dt, ³ J_{HH} = 6.5 Hz, ³ J_{HH} = 6.2 Hz, 12H), 1.56 (m, 12H), 1.45-1.22 (m, 60H), 0.91 (t, ³ J_{HH} = 6.8 Hz, 18H) ppm. ¹H NMR (250 MHz, CDCl₃): δ 9.51 (br s, 6H), 9.33 (s, 3H), 7.05 (s, 3H), 5.95 (s, 3H), 5.74 (s, 3H), 3.68 (br s, 6H), 3.01 (t, ³ J_{HH} = 7.0 Hz, 12H), 1.71-1.17 (m, 72H), 0.88 (t, ³ J_{HH} = 6.8 Hz, 18H) ppm. ¹³C NMR (63 MHz, CDCl₃): δ 146.7, 143.7, 129.5, 125.1, 121.6, 112.4, 95.7, 95.0, 44.2, 31.8, 29.5, 29.4, 29.2, 27.1, 22.6, 14.0 ppm. HRMS (ESI-TOF) *m/z*: [M+H]⁺ calcd. for C₈₄H₁₂₇N₁₈O₁₂⁺: 1579.9875, found 1579.9867, err. < 1 ppm. Single diffracting crystals of **4b** were obtained by cooling slowly a hot dimethylsulfoxide concentrated solution of **4b**.

Crystallography.

For **3b** intensity data of single crystal X-ray diffraction were collected on a Bruker–Nonius KappaCCD diffractometer using MoK α radiation (λ = 0.71073 Å). Data collection was performed with COLLECT,²² cell refinement and data reduction with DENZO/SCALEPACK.²³ For **4b** intensity data of single crystal X-ray diffraction were collected with a Rigaku Oxford Diffraction SpertNova diffractometer using Cu-K α radiation (λ = 1.54184 Å). The structures of **3b** and **4b** were solved with SIR92²⁴ and SHELXS²⁵ respectively while SHELXL2013²⁵ was used for full matrix least squares refinement. The hydrogen atoms were introduced at geometrical positions and their U_{iso} parameters were fixed to 1.2 U_{eq} (parent atom) for the aromatic or CH₂ carbon atoms and to 1.5 U_{eq} (parent atom) for the methyl groups. CCDC-1525759 (**3b**) and CCDC-1525760 (**4b**) contain the supplementary crystallographic data. These data can be obtained free of charge from The Cambridge

Crystallographic Data Centre via www.ccdc.cam.ac.uk/data_request.cif.

Computational details.

All (TD-)DFT calculations have been performed using the Gaussian 09.D01 program.²⁶ We have tightened both the self-consistent field (10^{-10} a.u.) and geometry optimization (10^{-5} a.u.) convergence thresholds and use an accurate (99,590) pruned DFT integration grid. The macrocycles have been modeled by replacing the C₈H₁₇ alkyl chains with Methyl groups. All our (TD-)DFT calculations relied on the PBE0 hybrid functional²⁷ using empirical dispersion corrections, as described by the so-called D3-BJ model.²⁸ CAM-B3LYP²⁹ was used to model the spectrum of the **4b**-C₆₀ complex as this functional is adequate for long-range charge-transfer phenomena. Following a basis set combination approach proposed previously,³⁰ we used the 6-31G(d) atomic basis set for determining the geometrical and vibrational parameters whereas the TD-DFT transition energies have been computed with 6-31+G(d,p) [6-31G(d) for the **4b**-C₆₀ complex]. In computing the conformation and interaction energies, single point calculations using the highly extended *def2*-QZVP basis set have been performed as well so to avoid the need of correcting for BSSE effects. The nature of all stationary points was confirmed by analytical Hessian calculations that returned 0 (minima) imaginary vibrational modes. These calculations gave access to estimates of the free energies (*G*). The NMR spectra were computed using the cc-pVTZ basis set. We note that the TMS reference signal was computed with the same protocol. Environmental effects [here, (CHCl₂)₂ for transitions and chloroform for NMR] have been accounted for electronic transition calculations, using polarizable continuum model (PCM),³¹ as implemented in Gaussian09,²⁶ applying the linear-response regime for excited-states. During the calculation of complexation and conformational energies, the solvent has also been introduced for single point calculation on the gas phase geometry using the PCM or SMD model.³²

Conclusions

Successive metal-free nucleophilic aromatic substitutions between an activated *meta*-dihalobenzene and a *meta*-diaminobenzene bearing two *n*-octylamino groups can lead to the concomitant and straightforward one-pot formation of the azacalix[6]arene **4b** and of the thermodynamically favoured azacalix[4]arene **3b**. Multiple analyses including single crystal X-ray diffraction, NMR and UV-Visible spectroscopy were combined with by TD-DFT calculations and put into evidence that both macrocycles feature a single conformer in solution which is the one observed in the crystalline solid state. If the corresponding 1,3-alternate conformer of the azacalix[4]arene **3b** was expected, the 1,2,4,5 alternate conformation adopted by the larger macrocycle **4b** has been rarely observed previously. This conformation remains flexible in solution and allows the formation of stable host-guest complexes between

the azacalix[6]arene **4b** and C60 which barely interacts with the smaller macrocycle **3b**.

Acknowledgements

This work was supported by the *Centre National de la Recherche Scientifique*, the *Ministère de la Recherche et des Nouvelles Technologies* (PhD grant to Z. C.) and the *Agence Nationale de la Recherche* in the frame of the EMA project (PhD grant of C. A.). D.J. thanks the LUMOMAT project for support. This works used computational resources of the IDRIS/CINES and of the CCIPL.

Notes and references

- 1 a) C. D. Gutsche, *Calixarenes: An Introduction*, The Royal Society of Chemistry, Cambridge, 2008; b) D. M. Homden and C. Redshaw, *Chem. Rev.*, 2008, **108**, 5086; c) Z.-Y. Li, J.-W. Chen, Y. Liu, W. Xia and L. Wang, *Curr. Org. Chem.*, 2011, **15**, 39; d) D. Semeril and D. Matt, *Coord. Chem. Rev.*, 2014, **279**, 58; e) N. Le Poul, Y. Le Mest, I. Jabin and O. Reinaud, *Acc. Chem. Res.*, 2015, **48**, 2097; f) J.-N. Rebilly, B. Colasson, O. Bistri, D. Over and O. Reinaud, *Chem. Soc. Rev.* 2015, **44**, 467; g) X. Ma and Y. Zhao, *Chem. Rev.*, 2015, **115**, 7794; h) M. Giuliani, I. Morbioli, F. Sansone and A. Casnati, *Chem. Commun.*, 2015, **51**, 14140.
- 2 B. König and Maria H. Fonseca, *Eur. J. Inorg. Chem.*, 2000, 2303.
- 3 a) P. Lhoták, *Eur. J. Org. Chem.*, 2004, 1675; b) N. Morohashi, F. Narumi, N. Iki, T. Hattori and S. Miyano, *Chem. Rev.*, 2006, **106**, 5291; c) R. Kumar, Y. O. Lee, V. Bhalla, M. Kumar and J. S. Kim, *Chem. Soc. Rev.*, 2014, **43**, 4824; d) F. Botha, V. Eigner, H. Dvořáková and P. Lhoták, *New J. Chem.*, 2016, **40**, 1104.
- 4 a) H. Tsue, K. Ishibashi and R. Tamura, *Top. Heterocycl. Chem.*, 2008, **17**, 73; b) M.-X. Wang, *Chem. Commun.*, 2008, 4541; c) M.-X. Wang, *Acc. Chem. Res.*, 2011, **45**, 182.
- 5 a) K. Ishibashi, H. Tsue, H. Takahashi and R. Tamura, *Tetrahedron: Asymmetry*, 2009, **20**, 375; b) M. Touil, J.-M. Raimundo, M. Lachkar, P. Marsal and O. Siri, *Tetrahedron*, 2010, **66**, 4377; c) Y. Yi, S. Fa, W. Cao, L. Zeng, M. Wang, H. Xu and X. Zhang, *Chem. Commun.*, 2012, **48**, 7495.
- 6 a) X. Z. Yan, J. Pawlas, T. Goodson, III and J. F. Hartwig, *J. Am. Chem. Soc.*, 2005, **127**, 9105; b) K. Ishibashi, H. Tsue, N. Sakai, S. Tokita, K. Matsui, J. Yamauchi and R. Tamura, *Chem. Commun.*, 2008, 2812; c) I. Kulszewicz-Bajer, V. Maurel, S. Gambarelli, I. Wielgus and D. Djurado, *Phys. Chem. Chem. Phys.*, 2009, **11**, 1362; d) A. Ito, *J. Mater. Chem. C*, 2016, **4**, 4614.
- 7 a) A. Ito, Y. Ono and K. Tanaka, *J. Org. Chem.*, 1999, **64**, 8236; b) Y. Miyazaki, T. Kanbara and T. Yamamoto, *Tetrahedron Lett.*, 2002, **43**, 7945; c) W. Fukushima, T. Kanbara and T. Yamamoto, *Synlett*, 2005, 2931; d) M. Vale, M. Pink, S. Rajca and A. Rajca, *J. Org. Chem.*, 2008, **73**, 27; e) Y.-X. Fang, L. Zhao, D.-X. Wang and M.-X. Wang, *J. Org. Chem.*, 2012, **77**, 10073.
- 8 a) M. Touil, M. Lachkar and O. Siri, *Tetrahedron Lett.*, 2008, **49**, 7250; b) J. Clayden, S. J. M. Rowbottom, W. J. Ebenezer and M. G. Hutchings, *Org. Biomol. Chem.*, 2009, **7**, 4871; c) H. Konishi, S. Hashimoto, T. Sakakibara, S. Matsubara, Y. Yasukawa, O. Morikawa and K. Kobayashi, *Tetrahedron Lett.*, 2009, **50**, 620; d) M. Xue and C.-F. Chen, *Org. Lett.*, 2009, **11**, 5294; e) R. Haddoub, M. Touil, J.-M. Raimundo and O. Siri, *Org. Lett.*, 2010, **12**, 2722; f) J. L. Katz and B. A. Tschaen, *Org. Lett.*, 2010, **12**, 4300; g) M. Touil, M. Elhabiri, M. Lachkar and O. Siri, *Eur. J. Org. Chem.*, 2011, 1914; h) R. Haddoub, M. Touil, Z. Chen, J.-M. Raimundo, P. Marsal, M. Elhabiri and O. Siri, *Eur. J. Org. Chem.*, 2014, 745; i) H. Xu, F.-J. Qian, Q.-X. Wu, M. Xue, Y. Yang and Y.-X. Chen, *RSC Adv.*, 2016, **6**, 27988.
- 9 J. W. Wackerly, J. M. Meyer, W. C. Crannell, S. B. King and J. L. Katz, *Macromolecules*, 2009, **42**, 8181.
- 10 V. Mehta, M. Panchal, K. Modi, A. Kongor, U. Panchal and V. K. Jain, *Curr. Org. Chem.*, 2015, **19**, 1077.
- 11 a) J. L. Katz, B. J. Geller and R. R. Conry, *Org. Lett.*, 2006, **8**, 2755; b) H. Konishi, K. Tanaka, Y. Teshima, T. Mita, O. Morikawa and K. Kobayashi, *Tetrahedron Lett.*, 2006, **47**, 4041.
- 12 a) W. Van Rossom, M. Ovaere, L. Van Meervelt, W. Dehaen and W. Maes, *Org. Lett.*, 2009, **11**, 1681; b) W. Van Rossom, K. Robeyns, M. Ovaere, L. Van Meervelt, W. Dehaen and W. Maes, *Org. Lett.*, 2011, **13**, 126.
- 13 F. Yang, L. Yan, K. Ma, L. Yang, J. Li, L. Chen and J. You, *Eur. J. Org. Chem.*, 2006, 1109.
- 14 a) M.-X. Wang, X.-H. Zhang and Q.-Y. Zheng, *Angew. Chem. Int. Ed.*, 2004, **43**, 838; b) H.-Y. Gong, X.-H. Zhang, D.-X. Wang, H.-W. Ma, Q.-Y. Zheng and M.-X. Wang, *Chem. Eur. J.*, 2006, **12**, 9262; c) E.-X. Zhang, D.-X. Wang, Q.-Y. Zheng and M.-X. Wang, *Org. Lett.*, 2008, **10**, 2565.
- 15 a) A.-J. Guan, E.-X. Zhang, J.-F. Xiang, Q. Li, Q.-F. Yang, L. Li, Y.-L. Tang and M.-X. Wang, *J. Phys. Chem. B*, 2011, **115**, 12584; b) A.-J. Guan, M.-J. Shen, J.-F. Xiang, E.-X. Zhang, Q. Li, H.-X. Sun, L.-X. Wang, G.-Z. Xu, Y.-L. Tang, L.-J. Xu and H.-Y. Gong, *Sci. Rep.*, 2015, **5**, 10479.
- 16 a) Z. Chen, M. Giorgi, D. Jacquemin, M. Elhabiri and O. Siri, *Angew. Chem. Int. Ed.*, 2013, **52**, 6250; b) G. Canard, J. A. Edzang, Z. Chen, M. Chessé, M. Elhabiri, M. Giorgi and O. Siri, *Chem. Eur. J.*, 2016, **22**, 5756.
- 17 Z. Chen, R. Haddoub, J. Mahé, G. Marchand, D. Jacquemin, J. Andeme Edzang, G. Canard, D. Ferry, O. Grauby, A. Ranguis and O. Siri, *Chem. Eur. J.*, 2016, **22**, 17820.
- 18 H. Tsue, K. Ishibashi, S. Tokita, H. Takahashi, K. Matsui and R. Tamura, *Chem. Eur. J.*, 2008, **14**, 6125.
- 19 Y. Suzuki, T. Yanagi, T. Kanbara and T. Yamamoto, *Synlett*, 2005, **2005**, 263.
- 20 P. Neri, M. Foti, G. Ferguson, J. F. Gallagher, B. Kaitner, M. Pons, M. A. Molins, L. Giunta and S. Pappalardo, *J. Am. Chem. Soc.*, 1992, **114**, 7814.
- 21 H. Tsue, K. Ishibashi, S. Tokita, K. Matsui, H. Takahashi and R. Tamura, *Chem. Lett.*, 2007, **36**, 1374.
- 22 COLLECT, Nonius BV, Delft, The Netherlands, 2001.
- 23 Z. Otwinowski and W. Minor, in *Methods in Enzymology. In Macromolecular Crystallography, Part A*, ed. C. W. Jr. Carter and R. M. Sweet, Academic Press: New York, 1997, vol. 276, p. 307.
- 24 A. Altomare, G. Cascarano, G. Giacovazzo, A. Guagliardi, M. C. Burla, G. Polidori and M. Camalli, *J. Appl. Crystallogr.*, 1994, **27**, 435.
- 25 G. M. Sheldrick, *Acta Crystallogr.*, 2008, **A64**, 112.
- 26 M. J. Frisch, G. W. Trucks, H. B. Schlegel, G. E. Scuseria, M. A. Robb, J. R. Cheeseman, G. Scalmani, V. Barone, B. Mennucci, G. A. Petersson, H. Nakatsuji, M. Caricato, X. Li, H. P. Hratchian, A. F. Izmaylov, J. Bloino, G. Zheng, J. L. Sonnenberg, M. Hada, M. Ehara, K. Toyota, R. Fukuda, J. Hasegawa, M. Ishida, T. Nakajima, Y. Honda, O. Kitao, H. Nakai, T. Vreven, J. A. Montgomery, Jr., J. E. Peralta, F. Ogliaro, M. Bearpark, J. J. Heyd, E. Brothers, K. N. Kudin, V. N. Staroverov, R. Kobayashi, J. Normand, K. Raghavachari, A. Rendell, J. C. Burant, S. S. Iyengar, J. Tomasi, M. Cossi, N. Rega, J. M. Millam, M. Klene, J. E. Knox, J. B. Cross, V. Bakken, C. Adamo, J. Jaramillo, R. Gomperts, R. E. Stratmann, O. Yazyev, A. J. Austin, R. Cammi, C. Pomelli, J. W. Ochterski, R. L. Martin, K. Morokuma, V. G. Zakrzewski, G. A. Voth, P.

- Salvador, J. J. Dannenberg, S. Dapprich, A. D. Daniels, O. Farkas, J. B. Foresman, J. V. Ortiz, J. Cioslowski and D. J. Fox, Gaussian 09 Revision D.01, 2009, Gaussian Inc. Wallingford CT.
- 27 C. Adamo, V. Barone, *J. Chem. Phys.*, 1999, **110**, 6158.
- 28 S. Grimme, S. Ehrlich, L. Goergik, *J. Comput. Chem.*, 2011, **32**, 1456.
- 29 T. Yanai, D. P. Tew, N. C. Handy, *Chem. Phys. Lett.*, 2004, **393**, 51.
- 30 B. Le Guennic., D. Jacquemin, *Acc. Chem. Res.*, 2015, **48**, 530, and references therein.
- 31 J. Tomasi, B. Mennucci, R. Cammi, *Chem. Rev.*, 2005, **105**, 2999.
- 32 A. V. Marenich, C. J. Cramer, D. G. Truhlar, *J. Phys. Chem. B*, 2009, **113**, 6378.